Phase retrieval with background compensation: variational inverse imaging technique for binary amplitude object

Artem Migukin
Department of Signal Processing, Tampere University of Technology
P.O. Box 527, 33101 Tampere, Finland
artem.migukin@tut.fi

March 30, 2012

Abstract

Traditionally the quality of wave field reconstructions obtained by phase-retrieval algorithms is poor: the object estimates are noisy and corrupted by various artifacts as blurring, irregular waves, spots, etc. The disturbances arising due to the wave field propagation in an optical setup are hard to be specified, but could be significantly suppressed by filtering. The contribution of this work concerns the compensation of these disturbances and wiping out typical distortions of the optical track by application of the adaptive sparse approximation so sharp object imaging to be achieved. This work is considered as a further development and improvement of the multi-plane phase-retrieval algorithm presented in [Migukin et al., Proc. SPIE **4829**, (2012)]. An advanced performance of the proposed algorithm is demonstrated for experimental data.

1 Introduction

The phase contains important information on the shape of the object, what is useful in metrology and 3D imaging, e.g. microscopy, astronomy, material analysis, etc. The conventional sensors detect only the intensity of the light. Since the phase cannot be measured directly and it is systematically lost in observations, computational phase recovering techniques are required for imaging and data processing. The conventional phase-retrieval techniques [1] are mainly based on the *ideal* wave field propagation modeling following, in particular, from the scalar diffraction theory [2]. In most cases wave fields in real coherent imaging systems and measured observations are quite different from the ones predicted by theory. The reconstructions obtained from the real data are corrupted by multiple and well seen artifacts which can have a form of disturbed background with irregular waves, spots, random

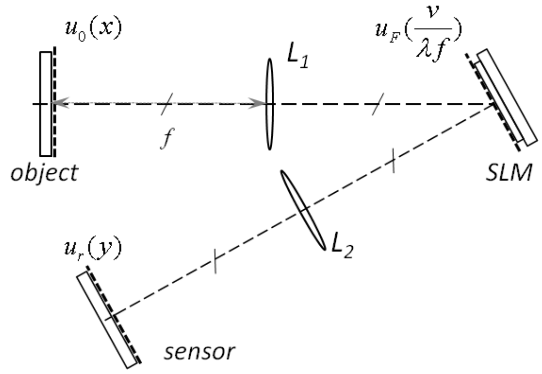

Figure 1: Experimental 4f optical setup for measurement recording [3]: The lenses L_1 and L_2 in the 4f configuration provides an accurate propagation of the object wave field to the parallel observation (sensor) plane. An optical mask (a phase modulating SLM) with the complex-valued transmittance $\mathbf{m}_r$ located at the Fourier plane enables linear filter operations.

noise, etc. These distortions appear due to many factors such as non-ideality of optical system (misalignment, focusing errors, aberrations), dust on optical elements, reflections, vibrations etc.

In this paper we consider 4f optical system with SLM in the Fourier domain of the first lens and use this system for the phase reconstruction from multiple intensity observations at the image plane (see Fig. 1, [3]). In this paper we do not try to identify particular sources of the disturbances but compensate their accumulated effect on reconstruction of the wave field at the entrance pupil of the 4f system.

Let $u_0(x)$, $x \in R^2$ be a true object wave field at the entrance pupil of the system. Taking into consideration the non-ideality of the optical system we introduce a corrupted object wave field $\tilde{u}_0(x)$ as a product of a typically unknown background (distortion) wave field u_B and the true object wave field $u_0(x)$

$$\tilde{u}_0(x) = u_0(x) \cdot u_B(x), \tag{1}$$

where the diacritic $\tilde{\cdot}$ emphasizes a difference of the real wave field $\tilde{u}_0$ from the ideal one u_0.

The standard phase retrieval techniques are able to give the reconstruction of the disturbed wave field $\tilde{u}_0(x)$ only and not able to separate the background in order estimate the true wave field $u_0(x)$. The motivation of this paper is developing of the procedure which is able to compensate background wave field using a simple calibration experiment with a fixed test-object $u_0(x) = c$. We consider the optimal wave field reconstruction, developed in terms of the variational constrained maximum likelihood formulation with parallel processing of multiple intensity observations. In the developed technique we mainly follow our previous works [4, 5] essentially modified in order to incorporate the results of the calibration experiments.

2 Observation model

We consider the image formation model in a conventional 4f configuration of the coherent imaging system linking complex amplitudes at the object and measurement planes. We use a vector-matrix notation for complex-valued distributions of the wave fields as $\mathbb{C}^{n\times 1}$ vectors, then $2D$ discrete distribution (matrix) of the size $M_x \times M_y$ is vectorized to the complex-valued column vector of the length $n = M_x \cdot M_y$. Bold lower case characters are used for the vectors. Matrices are defined by bold upper case to distinguish them from vectors. A reflective phase modulating spatial light modulator (SLM) is placed at the Fourier plane of the first lens. The forward wave field propagation from the object to the sensor plane can be given in the following simple form

$$\mathbf{u}_r = \mathbf{A}_r \cdot \tilde{\mathbf{u}}_0,\ r = 1, ...K, \tag{2}$$

where $\mathbf{u}_0$ and $\mathbf{u}_r$ are complex-valued vectors, corresponding to the discrete wave field distributions at the object and sensor planes, respectively. $\mathbf{A}_r \in \mathbb{C}^{n\times n}$ is a forward propagation operator presented as a transform matrix corresponding to the optical mask $\mathbf{m}_r$ on SLM. For simplicity in our numerical simulations we the images at the object, Fourier and sensor planes fo the same size $M_x \times M_y$.

We consider a multi-plane wave field reconstruction scenario, therefore K various transfer functions are programmed on SLM. Given a set of K experiments for different masks $\mathbf{m}_r$, $r = 1, ...K$ the problem is to reconstruct a complex-valued object wave field distribution from multiple noisy intensity observations $\{\mathbf{o}_r\}$ measured at the sensor plane

$$\mathbf{o}_r[k] = |\mathbf{u}_r[k]|^2 + \boldsymbol{\varepsilon}_r[k], r = 1, ...K \tag{3}$$

where the wave fields at the sensor plane are corrupted by the *background* due to non-ideality of the optical track (see Eq. (1)). We assume that the additive noise is zero-mean Gaussian $\boldsymbol{\varepsilon}_r[k] \sim \mathcal{N}(0, \sigma_r^2)$ with the standard deviation σ_r independent for various k and r.

3 Sparse modeling and variational formulation

Following [5] we represent the object wave field in the form $\mathbf{u}_0 = \mathbf{a}_0 \circ \exp(j \cdot \boldsymbol{\varphi}_0)$, where $\mathbf{a}_0 \triangleq |\mathbf{u}_0| \in \mathbb{R}^n$ and $\boldsymbol{\varphi}_0 \triangleq \arg\{\mathbf{u}_0\} \in \mathbb{R}^n$ denote the object amplitude and phase, respectively. In sparse modeling it is assumed that the true object distribution $\mathbf{u}_0$ can be approximated by a small number of non-zero elements $\boldsymbol{\theta}_a$ in the basis $\boldsymbol{\Psi}_a$ for the amplitude and $\boldsymbol{\theta}_\varphi$ in the basis $\boldsymbol{\Psi}_\varphi$ for the phase. Thus, the object reconstruction is performed by minimization of the criterion

$$J = \sum_{r=1}^{K} \frac{1}{2\sigma^2} ||\mathbf{o}_r - |\mathbf{u}_r|^2||_2^2 + \tau_a \cdot ||\boldsymbol{\theta}_a||_{l_p} + \tau_\varphi \cdot ||\boldsymbol{\theta}_\varphi||_{l_p} \tag{4}$$

$$\text{subject to } \mathbf{u}_r = \mathbf{A}_r \cdot \tilde{\mathbf{u}}_0,\ r = 1, ...K,$$

$$\boldsymbol{\theta}_a = \boldsymbol{\Phi}_a \cdot |\mathbf{u}_0|, \boldsymbol{\theta}_\varphi = \boldsymbol{\Phi}_\varphi \cdot \arg\{\mathbf{u}_0\},\ \mathbf{u}_0 = \boldsymbol{\Psi}_a \boldsymbol{\theta}_a \circ \exp(j \cdot \boldsymbol{\Psi}_\varphi \boldsymbol{\theta}_\varphi)$$

where regularization terms for phase and amplitude are taken using the l_p norms ($p = \{0, 1\}$). $\boldsymbol{\Psi}.$ and $\boldsymbol{\Phi}.$ are the frame transform matrices, and the vector $\boldsymbol{\theta}. \in \mathbb{R}^m$ can be considered as a spectrum ($m \gg n$) in a parametric data adaptive approximation (subindices a and φ are shown for the amplitude and phase, respectively). The positive parameters τ_a and τ_φ define a balance between the fit of observations, smoothness of the wave field reconstruction and the complexity of the used model (cardinality of spectra $\boldsymbol{\theta}_a$, $\boldsymbol{\theta}_\varphi$ of the object amplitude and phase). The separate sparse modeling for the object phase and amplitude is realized via the powerful BM3D-frame filter, specified for denoising and other imaging problems [6].

4 Numerical experiments

In our numerical experiments we consider the reconstruction of the amplitude-only binary object wave field distribution $\mathbf{u}_0[k] = \mathbf{a}_0[k]$ with a standard USAF 1951 test-chart as $\mathbf{a}_0$, $\boldsymbol{\varphi}_0[k] = 0$. Following to the approach described by Falldorf et al. in [3], the SLM is used in order to imitate free-space wave field propagation in terms of the angular spectrum decomposition [2]. We program on SLM K=5 various transfer functions $\mathbf{m}_r$, $r = 1, ...K$ corresponding to different propagation distances z_r.

The advantage of the background compensation by the proposed phase-retrieval algorithm can be easily demonstrated by the numerical simulations ($M_x \times M_y = 1296 \times 1296$). First, the optical distortions in the coherent imaging system are modeled with a synthetic amplitude-only smooth $\mathbf{u}_B \in \mathbb{R}^n$ demonstrated in Fig. 2(b).

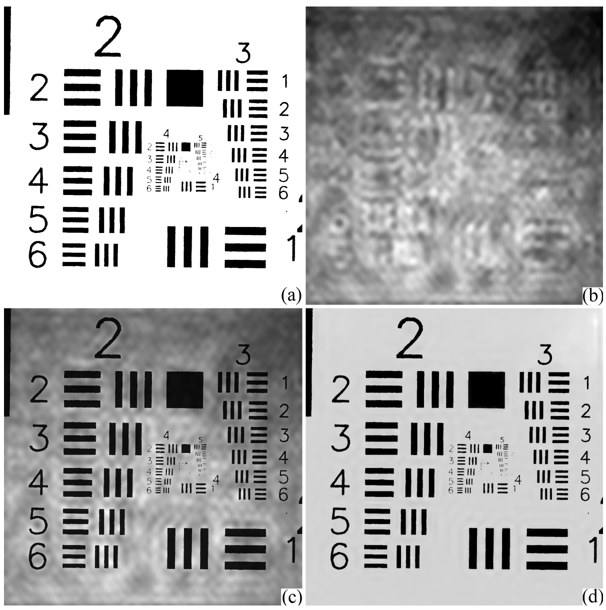

Figure 2: Modeling results of the proposed phase retrieval with background compensation: (a) a test image used as the amplitude-only $\mathbf{u}_0 = \mathbf{a}_0$, (b) a synthetic amplitude-only smooth background $\mathbf{u}_B$, (c) the estimate of the corrupted object amplitude $|\tilde{\mathbf{u}}_0|$ found by AL, RMSE=0.4, (d) the reconstructed amplitude estimate $|\hat{\mathbf{u}}_0|$ found by the proposed algorithm, RMSE=0.043.

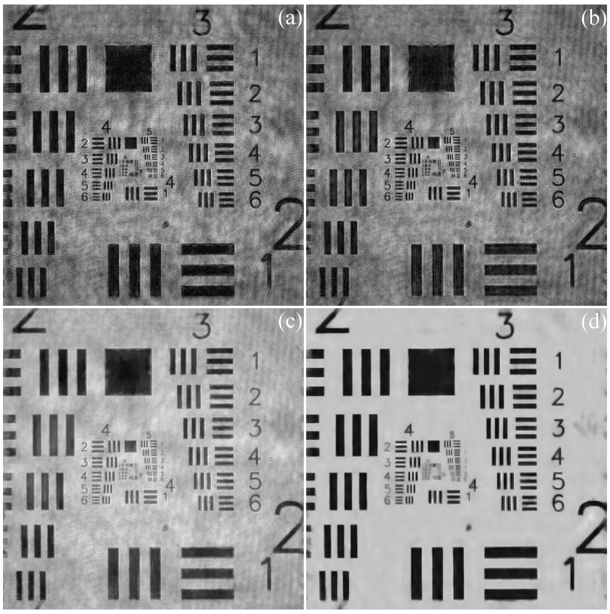

Figure 3: Reconstructions of the object amplitude from experimental data, obtained by (a) $SBMIR$ [8], (b) AL [4], (c) $D-AL$ [5] with over-smoothing, and (d) the proposed algorithm with background compensation.

The background is constructed from a corrupted object amplitude estimate with inpainting of geometrical elements by Criminisi's algorithm [7] and blockwise linear regression for smoothing. We construct a number of noisy intensity observation representing the disturbances of the coherent imaging system for a flat signal $\mathbf{u}_0[k]=1$ and find the complex-valued estimate of the background $\hat{\mathbf{u}}_B$ by AL [4]. Then, the test image used in our numerical simulations as the true signal $\mathbf{a}_0$ is illustrated in Fig. 2(a). According to the used observation model we obtain the observations for $\mathbf{a}_0 \circ \mathbf{u}_B$.

In Figs. 2(c) and 2(d) the amplitude estimates of $\tilde{\mathbf{u}}_0$ and $\mathbf{u}_0$ computed by AL and the proposed algorithm with background compensation, respectively are shown. The visual advantage of the proposed algorithm is obvious: the compensation of the background lead to a significantly improvement of imaging. The background estimate "undertakes" strong fluctuations, which would be difficult to compensate by filtering. The wave field reconstruction accuracy is found by root-mean-square error (RMSE). RMSE for the estimate of the corrupted object amplitude $|\tilde{\mathbf{u}}_0|$ (Fig. 2(c)) is approximately 0.4 and RMSE for $|\hat{\mathbf{u}}_0|$ (Fig. 2(d)) is 0.043.

4.1 Reconstruction from experimental data

In Fig. 3 we present some numerical results of the reconstructed amplitudes from the experimental data obtained according to the 4f model [3]. The the measurements are obtained in the Bremen Institute of Applied Beam Technology (BIAS) by Dr. Mostafa Agour.

We reconstruct only a part of the object estimate of the size $M_x \times M_y = 2048 \times$

2048. In Fig. 3 we compare the reconstruction imaging of the object obtained from experimental data by different methods. In Fig. 3(a) the estimate of the object amplitude $|\hat{\mathbf{u}}_0|$ calculated by $SBMIR$ [8] is presented. Fig. 3(b) demonstrates the amplitude reconstruction by AL. It can be seen that the fluctuations (especially on the borders), are partially suppressed. The amplitude estimate found using the $D-AL$ algorithm [5] is shwn in Fig. 3(c) with some modification of the BM3D-frame filter, what result in a better suppression of "waves", but the image contrast is worse. The best imaging is presented in Fig. 3(d) by the proposed algorithm. Note that no image adjustment as gamma correction is produced for the imaging. These results are shown for 25 iterations of the phase-retrieval algorithms.

References

[1] J. R. Fienup, "Phase retrieval algorithms: a comparison," Appl. Opt. **21**, 2758-2769 (1982).

[2] J. W. Goodman, *Introduction to Fourier Optics*, 2nd ed. (McGraw-Hill, 1996).

[3] C. Falldorf, M. Agour, C. v. Kopylow, and R. B. Bergmann, "Phase retrieval by means of a spatial light modulator in the Fourier domain of an imaging system," *Appl. Opt.* **49**, 1826 – 1830 (2010).

[4] A. Migukin, V. Katkovnik, and J. Astola, "Wave field reconstruction from multiple plane intensity-only data: Augmented Lagrangian algorithm", J. Opt. Soc. Am. A **28**, 993–1002 (2011).

[5] A. Migukin, V. Katkovnik, and J. Astola, "Advanced multi-plane phase retrieval using Graphic Processing Unit: augmented Lagrangian technique with sparse regularization," Proc. SPIE 8429, (2012), in press.

[6] V. Katkovnik, A. Danielyan, and K. Egiazarian, "Decoupled inverse and denoising for image deblurring: variational BM3D-frame technique," in *Proceedings of the International Conference on Image Processing* (ICIP), 3514 – 3517 (2011).

[7] A. Criminisi, P. Perez, and K. Toyama, "Object removal by exemplar-based inpainting," CVPR'03, (2003).

[8] G. Pedrini, W. Osten, and Y. Zhang, "Wave-front reconstruction from a sequence of interferograms recorded at different planes," Opt. Lett. **30**, 833-835 (2005).